

Photokilling of *Escherichia coli* Using Hybrid Titania Nanoparticles Suspended in an Aqueous Liquid

Christophe Massard¹, Muriel Bonnet², Philippe Veisseire², Yves Sibaud¹, Eric Caudron¹,
Komla Oscar Awitor¹

¹Clermont Université, Université d'Auvergne, C-BIOSENS EA-4676 Clermont-Ferrand, France; ² Clermont Université, Université d'Auvergne, Laboratoire de Biologie, IUT Génie Biologique, Aurillac, France.
Email: christophe.massard@udamail.fr

Received January 17th, 2013; revised March 2nd, 2013; accepted April 5th, 2013

Copyright © 2013 Christophe Massard *et al.* This is an open access article distributed under the Creative Commons Attribution License, which permits unrestricted use, distribution, and reproduction in any medium, provided the original work is properly cited.

ABSTRACT

In this work, the photokilling of *Escherichia coli* using a “one-pot” synthesized suspension of anatase crystallized nanoparticles is evaluated. Preliminary to the biological tests concerning the antibacterial efficiency, the fabricated suspension, using a derived sol-gel process in soft chemistry condition, is characterized. Structural properties of the nanoparticles are investigated using Electronic Transmission Microscopy (TEM) equipped with Selected Area Electron Diffraction (SAED) probe and X-ray diffraction. The inorganic solid content was evaluated by Thermogravimetric Analysis (TGA). Photodegradation of Acid Orange 7 in aqueous solution was used as a probe to assess the photocatalytic activity of the elaborated suspension under UV irradiation. The photokilling of *Escherichia coli* in presence of hybrid TiO₂ nanoparticles suspended in aqueous liquid under UV irradiation is evaluated. Such TiO₂ nanoparticles suspension shows a strong bactericidal activity with the total destruction of bacteria after only one hour.

Keywords: Anatase TiO₂; Photocatalysis; Sol-Gel; Bacteria; Photokilling; *Escherichia coli*

1. Introduction

New technologies for disinfection applications are a growing market nowadays. Alternative process to conventional disinfection methods are required to meet the new requirements of health care regulations in numerous applications. Concerning the water disinfection, the use of free chlorine as a disinfectant of ground water containing a high rate of organic species induces the genesis of disinfection by-products (DBS) hazardous to human health [1-3]. Medical applications also require high efficiency and none hazardous sterilization process. Surgery devices surfaces are colonized by bacteria [4-6]: the emergence of resistant and virulent strains of micro-organism combined to the wide spread use of antibiotics necessitate new disinfection technologies. Disinfection of areas of intensive medical use or laboratories surfaces is essential for the biological security [7]. The manual disinfection by wiping using aggressive chemicals is not efficient enough and may cause troubles to the people. The use of TiO₂ nanoparticles in suspension as a photocatalytic disinfection device seems to be an interesting alternative to conventional process. No expensive or danger-

ous chemicals are needed, and high disinfection efficiency can be reached, combined to the mineralization of the organic species. Many studies have reported the efficiency of photocatalysis for destroying microorganisms in water. Extensive research has been done about the destruction of *E. coli* using TiO₂ suspension and TiO₂ films [8-12]. This bactericidal effect of nanoparticles was explained either by disruption of cell membrane activity [13,14] or induction of intercellular reactive oxygen species, including hydrogen peroxide (H₂O₂), superoxide (O₂⁻) and hydroxyl radical (HO[•]) strong oxidizing agents harmful to bacterial cells [13,15]. In this study, we investigate both the physico-chemical properties of our synthesized suspension of anatase crystallized TiO₂ nanoparticles and the inactivation of *Gram-negative Escherichia coli* (strain LE392) by a photokilling process.

2. Materials and Methods

2.1. Nanoparticles Suspension Synthesis

The precursor solution was 10 mL titanium IV isopropoxide 97% supplied by ©Sigma Aldrich mixed with 10 mL of anhydrous isopropanol (from ©Sigma) under a vi-

gorous stirring. The titanium alkoxide reactivity is lowered by the use of acetylacetone as chelating reagent. The spontaneous hydrolysis of the titanium isopropoxide is obtained by the quick addition of 75 mL of acidified water. The reacting medium is then heated to 80°C under reflux for almost 8 hours (peptidization process). After this step, the dispersion is cooled down to room temperature. A clear, yellow, nanoparticles suspension is obtained.

2.2. X-Ray Diffraction Analysis

XRD measurements are performed on the ©Philips x'pert MPD diffractometer operating in the reflection mode with Cu-K α 1 radiation (1.5406 Å, 40 kV, 55 mA) and diffracted beam monochromator, using a step scan mode with a step of 0.1° (2 θ) and 3 s per step. Diffraction pattern obtained from the TiO₂ nanopowder is compared with reference to the Joint Committee on Powder Diffraction Standards (JCPDS) database.

2.3. Transmission Electron Microscopy

The morphology and the particles sizes were characterized using a ©Philips CM 20 transmission electron microscope (TEM). The accelerating voltage was 200 kV. The samples were dispersed in methanol by ultra sonication. A drop of the suspension was then laid on a carbon-coated grid and dried. Selected Area Electron Diffraction (SAED) was performed to determine the crystallinity of the structure. The interplanar spacings were measured from the SAED patterns using Equation (1):

$$\lambda L = R d \quad (1)$$

where λL is a constant of the microscope, R is the ring radius, and d is the interplanar distance. The constant of the microscope was calculated by measuring the radius of a gold standard pattern which interplanar distances are well documented in literature.

2.4. Thermogravimetric Analysis

The thermogravimetric analysis was carried out using the TGA 4000 thermogravimetric analyser (©Perkin Elmer instrument). The analysis was performed at a heating rate of 5°C·min⁻¹ under a 40 mL·min⁻¹ nitrogen gas flow. Prior to the TGA tests, a designated volume of 20 mL of the TiO₂ suspension was dried at 110°C overnight.

2.5. Photocatalytic Activity Study

Photodegradation of an organic dye, Acid Orange 7 supplied by ©Acros-Organic (AO7) in aqueous solution was used as a probe to assess the photocatalytic activity of the TiO₂ suspension.

The experiments were carried out using 3 mL of AO7 solution (5×10⁻⁵ mol·L⁻¹). In order to avoid the dilution

effect, 60 μ L of the TiO₂ suspension was added to the 3 mL of the organic dye solution under stirring at 200 rpm. After homogenization, the mixture was irradiated in an air-cooled cylindrical reactor under stirring with polychromatic fluorescent UV lamps (©Philips TLD 8W) providing a total power of 48 W, in a configuration delivering about 0.8 mW·cm⁻² at the liquid surface. Each sample was irradiated one time and replaced by a new one to avoid cumulative effect.

The UV induced degradation of the organic dye was recorded from 200 to 700 nm with a resolution of 2 nm using a ©Perkin Elmer Lambda 35 spectrometer. Quartz glass cells with an optical pathway of 1 cm were used. De-ionized water was taken as reference. The reaction was followed by monitoring the decrease of the solution's absorbance at 483 nm (strong absorption band of the Acid Orange 7).

2.6. Bacterial Culture

Escherichia coli LE392 was used as a model micro-organism for photokilling experiments. Bacteria cells were cultured at 37°C for 12 h in Nutrient Broth medium at pH 7.2 (Biokar Diagnostics) containing Tryptone (10 g·L⁻¹), Meat extract (5 g·L⁻¹) and Sodium Chloride (5 g·L⁻¹) after 12 h of pre-culture in the same conditions. Cells were centrifuged at 2500 g for 15 min at 4°C and the pellet was re-suspended in de-ionized water to prevent unintentional increase in cell numbers. The initial population of *E. coli* was determined by enumeration with a Petroff-Hausser Counting Chamber.

2.7. Photokilling Measurements

An amount of 20 ml of de-ionized water was inoculated with *E. coli* suspension in order to achieve a concentration of 10⁶ cfu·mL⁻¹. This culture was placed in a Petri plate and TiO₂ nanoparticles, either in nanopowder form or suspended in the carrying liquid, were added to achieve a final concentration in TiO₂ of 1 g·L⁻¹. The slurries were continuously mixed with a sterilized Teflon magnetic stir bar placed in the Petri dish with a speed of 200 rpm to allow a complete mixing.

In order to investigate the potential toxicity of the carrying liquid in which the TiO₂ nanoparticles were suspended, measurements were performed on the mixture composed of *E. coli* suspension and the designed volume of carrying liquid without TiO₂ nanoparticles. Chemical composition of the carrying liquid is described in **Table 1**.

All experiments were made in Petri dishes and the different experimental conditions are presented in **Table 2**.

Irradiation was provided by polychromatic fluorescent UV lamps (©Philips TLD 8W) providing a total power of 48 W, in a configuration delivering 1.5 mW·cm⁻² at

Table 1. Chemical composition of the carrying liquid in which the TiO₂ nanoparticles are suspended.

Chemical reagent	Weight %
Deionized water	84
Isopropyl alcohol	10
Acetylacetone	6

Table 2. Different assays realized with the TiO₂ nanopowder from the synthesis and the synthesized TiO₂ nanoparticles suspension. C = *E. coli* suspension in the dark; NP = *E. coli* suspension in presence of the TiO₂ nanopowder from the synthesis or synthesized TiO₂ nanoparticles suspension. UV = *E. coli* irradiated with UV light; S = *E. coli* suspension with the carrying liquid; SUV = *E. coli* suspension irradiated with UV light in presence of the carrying liquid; NPUV = *E. coli* suspension irradiated with UV light in presence of nanoparticles.

	C	NP	UV	S	SUV	NPUV
TiO ₂ nanopowder	X	X	X			X
TiO ₂ nanoparticles suspension	X	X	X	X	X	X

the liquid surface. Sampling of the solutions was done at requisite time intervals by pipetting 1 mL from the suspension and serially diluted in 9 mL of Ringer's solution. After well mixing, 100 μ L aliquots of each dilution were plated onto solid Nutrient Gelose medium (Agar 1.5 g·L⁻¹). Colony-forming units were counted after overnight incubation at 37°C. All experiments were made in aseptic conditions to prevent any contamination in mediums. The counts from three independent experiments corresponding to a particular sample were averaged.

3. Results and Discussions

3.1. Titania Nanoparticle Synthesis

Crystalized TiO₂ nanoparticles in suspension were successfully synthesized by chelation and hydrolysis-condensation of the titanium alkoxide precursor. The synthesis included a low temperature protocol which is a significant advantage compared to the others requiring high temperature to obtain crystalized phase [16,17]. Another advantage is that the stable suspension obtained avoids the use of potentially toxic dry nanopowder. Studies are dealing with the research of the suspensions' stability and their biological behavior [18]. The process followed induces high stability of the suspension and opens the way to develop interesting photocatalytic process. The chemical functionalization of the titanium alkoxide by a beta diketone is a substitution of alkoxy group by a less hydrolysable one such as acetylacetone. This chelation slows down the hydrolysis kinetic, avoids undesired precipitate and promotes the dispersion of the colloids in the

liquid.

3.2. X-Ray Diffraction on the TiO₂ Nanopowder

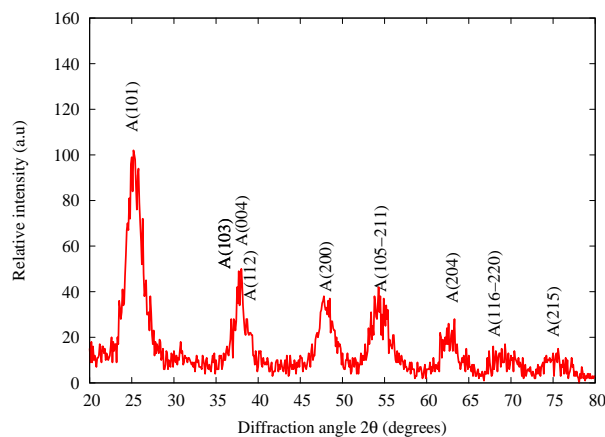
X-ray diffraction of the dried nanopowder is shown in **Figure 1**. XRD pattern exhibits strong diffraction peaks at 25°C and 38°C indicating TiO₂ in the anatase phase. All peaks present are in good agreement with the standards spectrum (JCPDS n.: 21-1272). The crystallite size, D, is evaluated by measuring the width of the curves produced and using the Scherrer formula (2):

$$D = \frac{(0.9 * \lambda)}{\beta \cos(\theta)} \quad (2)$$

where λ is the wavelength of the Cu K_{α1} line in nm, β is the full-width at half max (FWHM) of the peak. Using the FWHM of the (101) anatase peak, we found that the average crystal size was about 8 nm.

3.3. Transmission Electron Microscopy

A typical TEM image of the as-synthesized TiO₂ nanoparticles is presented in **Figure 2(a)**. The particles are flake-shaped and tend to agglomerate to form aggregates but less than reported in the case of nanopowder [19]. This well-dispersed situation is attributed to the chemical functionalization of the surface which acts as surfactant and promotes the individualization of the particles. Generally speaking, the agglomeration tendency is explained by the fact that the new state is more stable in the energetic point of view and allows the crystallite growth. The different TEM images of our study are consistent with a well-dispersed suspension of nanoparticles. From these pictures, the crystallite size is between 7 and 20 nm. The SAED pattern of the nanoparticles is shown in **Figure 2(b)**. A comparison between the interplanar distances calculated from the SAED pattern and the tabulated ones for the TiO₂ anatase crystallographic structure

**Figure 1. X-ray diffraction of the TiO₂ grafted acetylacetone nanopowder.**

reveals a high degree of consistency (Table 3). This comparison reveals the polycrystalline nature of our sample. The interplanar spacings measured correspond to the TiO₂ anatase structure. This study confirms the results obtained by the XRD analysis on the nanopowder and validates our synthesis approach: a stable suspension of TiO₂ anatase nanoparticles in aqueous medium is obtained.

3.4. Thermogravimetry Study

Table 4 gives the characteristics of the samples analysed by TGA. Sample S2 was used as a reference for TiO₂ nanopowder without organic components. Sample S1 was the organic functionalized TiO₂ nanopowder from the suspension. TGA measurements were carried out from 50°C to 1000°C at a heating rate of 5°C·min⁻¹.

Figure 3 shows the TGA curves.

As far as the manufactured TiO₂ nanopowder is concerned, no significant weight loss is recorded in the 100°C - 1000°C range. In comparison, the weight loss curve of the organic functionalized TiO₂ nanopowder exhibits two significant weight losses. The first one occurs in the 100°C - 200°C range and is attributed to the desorption of volatile compound such as residual water and

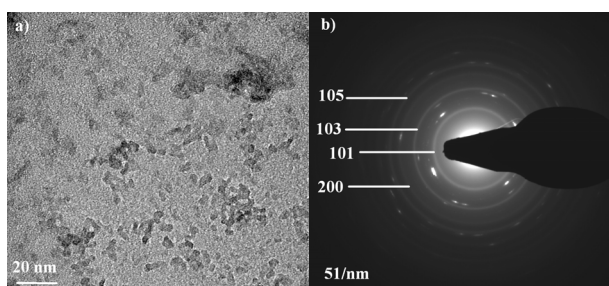


Figure 2. TEM image of TiO₂ nanoparticles (a) and SAED pattern of the particles (b).

Table 3. Interplanar distances for the TiO₂ nanoparticles deduced from the SAED patterns, compared to the expected ones for ideal anatase phase.

Interplanar distance from the SAED pattern (Å)	3.57	2.41	1.93	1.70
Theoretical distance for the anatase phase (Å)	3.51	2.33	1.89	1.66
Corresponding Miller indice	(101)	(103)	(200)	(211)

Table 4. Samples characteristics analyzed by TGA.

Sample identification	Charateristics	Weight	Drying condition
S1	nanopowder from the synthesis	19.1 mg	110°C overnight
S2	nanopowder from Sigma Aldrich	20 mg	none

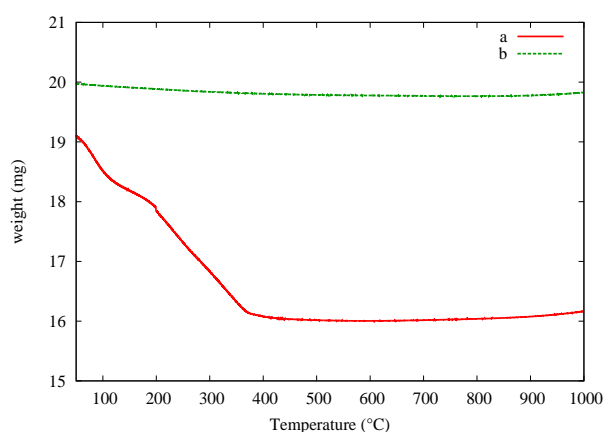


Figure 3. TGA curves of the TiO₂ grafted acetylacetonate nanopowder from the synthesis (a) and pure TiO₂ used as a reference (b).

alcohol. The second weight loss in the 200°C - 380°C range is correlated with the progressive thermal degradation of the grafted acetylacetonate group on the TiO₂ nanoparticles surface. The pyrolysis of the organic surfactant is taken up to 450°C. At the highest temperature, in our analytical conditions, no more weight loss is recorded, so pure inorganic TiO₂ nanopowder is obtained. A comparison between the samples leads to a total estimated weight loss around 16 wt%. The theoretical suspension concentration is estimated considering the initial amount of precursor and the volume of liquid. This result leads to a calculated estimation of TiO₂ concentration in the dispersion around 27 mg·mL⁻¹ or 16400 ppm in titanium. This theoretical result is in good agreement with the experimental value given by TGA.

3.5. Photocatalytic Results

Preliminary, a study of the homogenization of the mixture has been done without irradiation. A volume of 60 µL of the TiO₂ suspension was added to 3 mL of AO7 solution (5 × 10⁻⁵ mol·L⁻¹). The influence of the stirring time at 200 rpm on the solution homogeneity is summarized in Figure 4. First, by comparison between Figures 4(a) and (b), we evidenced that the addition of TiO₂ suspension has a high impact on the AO7 solution's absorbance at an analytical wavelength of 483 nm. The AO7 solution's absorbance was decreased nearly to 35% when the TiO₂ particles were loaded in the solution. Strong adsorption effect between the organic dye and the nanoparticles may explain this decrease in absorbance. We evidenced that 5 minutes of stirring is required to stabilize the solution's absorbance. A longer stirring time has no effect when we compare the curves Figures 4(c) (5 minutes of stirring) and (d) (30 minutes of stirring). Accordingly to these preliminaries investigations, all our photocatalytic experiments were carried out after a ho-

mogenization step of 5 minutes of stirring at 200 rpm without UV irradiation. The stirring speed remained constant in all the experiments.

The photodegradation behavior of the AO7 solution in presence of nanoparticles was investigated under different conditions summarized in **Figure 5**.

The AO7 concentration versus the irradiation time was determined by the absorbance's measurement at the analytical wavelength of 483 nm. **Figure 5** curve (a) shows the UV-photodegradation of the AO7 solution ($5 \times 10^{-5} \text{ mol}\cdot\text{L}^{-1}$) without TiO_2 suspension. No significant UV photodegradation is recorded as the solutions concentration remains unchanged during the irradiation. **Figure 5**

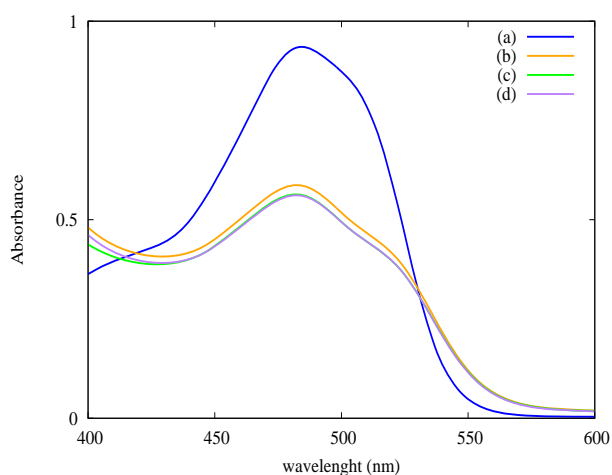


Figure 4. Impact of the stirring time at 200 rpm without UV irradiation on the solution's absorbance at 483 nm: (a) AO7 only; (b) AO7 and TiO_2 suspension without stirring; (c) AO7 and TiO_2 suspension, 5 minutes stirring; (d) AO7 and TiO_2 suspension, 30 minutes stirring.

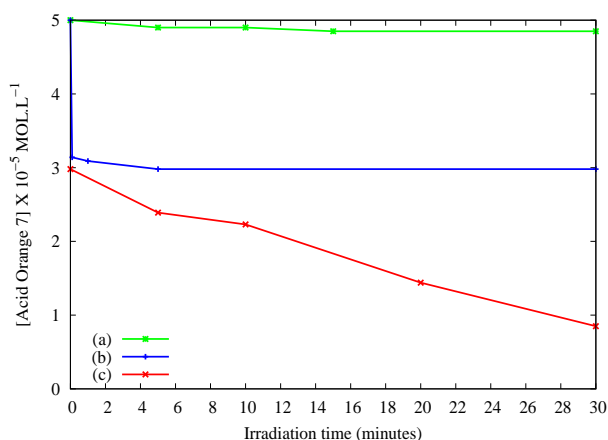


Figure 5. Photodegradation of the Acid Orange 7 solution in the presence of TiO_2 nanoparticles under UV irradiation as measured by the solution's absorbance at $\lambda = 483 \text{ nm}$: (a) AO7 only under UV irradiation; (b) AO7 and TiO_2 suspension without UV irradiation; (c) AO7 and TiO_2 suspension, under UV irradiation.

curve (b) exhibits that the concentration's reduction is about 35% without UV curing after 5 minutes of stirring with the designed volume of TiO_2 suspension. As previously discussed, the interaction between the organic dye and the particles may explain this decrease. **Figure 5** curve (c) highlights the variation in concentration of AO7 with TiO_2 nanoparticles under UV irradiation. A quick decrease of the solution's concentration is evidenced. A complete decolorization of the solution was observed after 30 minutes of irradiation. These results show the photocatalytic activity of the TiO_2 nanoparticles dispersed in the organic dye solution. This efficiency is attributed to the anatase crystalline structure of our nanoparticles and to their high specific surface. Compared to previous works published elsewhere [20,21], the photodegradation kinetic is improved by the establishment of a macroscopic liquid/liquid interface compared to a solid/liquid counterpart. The reproducibility of the results was tested by repeating the measurements. **Figure 6** shows the absorbance spectra for 10 minutes of UV irradiation.

The curves concerning the exposure of the AO7- TiO_2 mixture with the same UV irradiation time duplicated on two different samples are superimposed, revealing a good reproducibility of the protocol used and validating the method of following the degradation of Acid Orange 7 by the use of UV spectrometry.

3.6. Antibacterial Efficiency Study

Figure 7 shows the effect of our TiO_2 nanopowder from the synthesis on *Escherichia coli* under UV irradiation. Firstly, the result demonstrates that the ultraviolet light used in this experiment did not affect significantly the viability of bacteria after 3 hours in absence of TiO_2

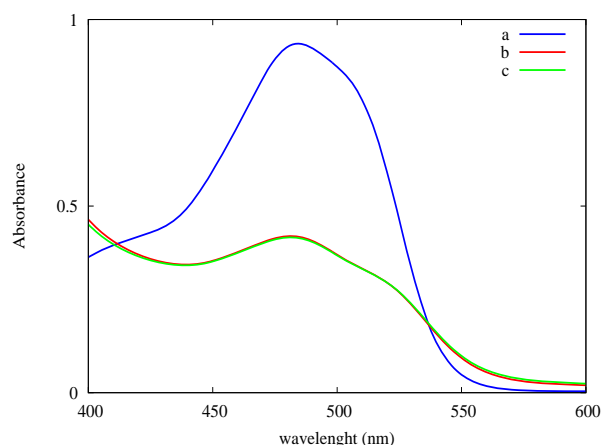


Figure 6. Reproducibility test of the photodegradation of the Acid Orange 7 solution under UV irradiation as measured by the solution's absorbance at $\lambda = 483 \text{ nm}$: (a) AO7 only under UV irradiation; (b) AO7 and TiO_2 suspension after 10 minutes of UV irradiation; (c) AO7 and TiO_2 suspension, after 10 minutes of UV irradiation (duplicate).

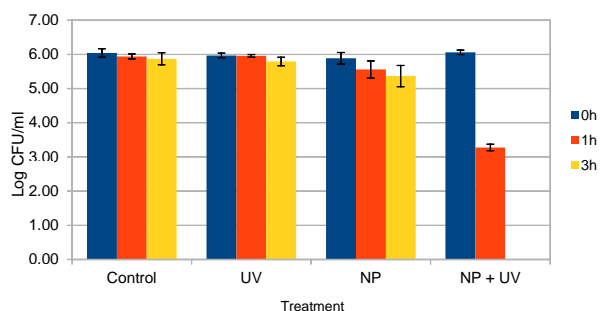


Figure 7. The growth of bacteria after our experimental conditions with our TiO₂ nanopowder from our synthesis. Control = *E. coli* suspension alone in the dark; UV = *E. coli* under UV light; NP = *E. coli* suspension with 1 g·L⁻¹ TiO₂ nanopowder in the dark; and NP + UV = *E. coli* suspension under UV light in presence of 1 g·L⁻¹ TiO₂ nanopowder. Error bars represent standard deviation from the mean, n = 3.

nanoparticles. Secondly, in the absence of UV light all bacteria survived well in the presence of TiO₂ nanopowder during all the experiment, *i.e.* 3 hours of treatment. Finally, when the population of *E. coli*, was in contact with TiO₂ nanoparticles (1 g·L⁻¹) under UV irradiation for one hour, the living bacteria decreased approximately near 3 logs. After 3 hours of irradiation in presence of TiO₂ nanopowder, bacteria were completely killed. These results confirm the bactericidal effect of TiO₂ nanopowder published elsewhere [22-24].

In order to discriminate the effect of the carrying liquid and TiO₂ nanoparticles in suspension on the bacterial death, measurements were done with the carrying liquid alone and with the TiO₂ nanoparticles in suspension in the carrying liquid (**Figure 8**).

The results show that no significant effect was detected with the carrying liquid alone on survival of bacteria during all the experiment, so our carrying liquid has a low toxicity unlike to pure organic solvent [25]. This result could be explained by the low concentration of acetylacetone used in our carrying liquid (6 wt%) (**Table 1**). Nevertheless, the number of survival bacteria decreased of approximately 1 log after 3 hours of exposure while the carrying liquid alone is under UV irradiation. This behavior can be explained by photoisomerization of acetylacetone in presence of UV light, leading to a production of nonchelated isomers [26] which can be toxic molecules for the micro-organism. We underline the fact that our experiments concerning the evaluation of the toxicity of the carrying liquid lead to an overestimation of its real toxicity, assuming the fact that the acetylacetone molecular species are less reactive in the suspension because of their chemical grafting onto the titanium alcoxide.

In order to compare the efficiency in bactericidal effect of TiO₂ nanoparticles in suspension, we assessed a similar experiment using our suspension of TiO₂ nano-

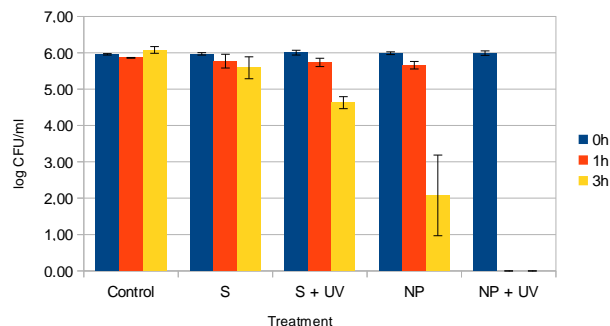


Figure 8. The growth of bacteria after our experimental conditions with suspension of TiO₂ nanoparticles. Control = *E. coli* suspension alone in the dark; S = *E. coli* suspension with 1 g·L⁻¹ carrying liquid S + UV = *E. coli* suspension with 1 g·L⁻¹ carrying liquid, in presence of UV light; NP = *E. coli* suspension with 1 g·L⁻¹ TiO₂ nanoparticles in suspension and NP + UV = *E. coli* suspension under UV irradiation in presence of 1 g·L⁻¹ TiO₂ nanoparticles in suspension. Error bars represent standard deviation from the mean, n = 3.

particles at the same concentration of 1 g·L⁻¹ (**Figure 8**).

In comparison with the use of TiO₂ nanopowder (**Figure 7**), in the dark, an important death of bacteria was observed when they were exposed with the nanoparticles suspended in the carrying liquid for 3 hours (**Figure 8**). Effectively, the bacteria population was diminished from 6 logs to 2 logs, whereas no effect was detected with our TiO₂ nanopowder after the same duration. This demonstrates that nanoparticles, when dispersed in the carrying liquid, in the dark, have a fair killing activity on bacteria. Moreover, the photokilling effect on *E. coli* was more effective with the TiO₂ suspension in the carrying liquid than the nanopowder of TiO₂ when the population was submitted to UV irradiation. In this particular condition, we clearly observed the total destruction of bacteria after only 1 hour. This greater inhibition in the presence of UV light supports the notion that the antibacterial activity is related to a more efficient surface of contact between TiO₂ nanoparticles in suspension and bacteria than TiO₂ nanopowder and bacteria. TiO₂ nanopowder aggregates and settles quickly, resulting in smaller surface of contact so in more limited production of photocatalytic reactive oxygen species. Indeed, TiO₂ nanoparticles induced radical oxygen species generation and glutathione depletion, accompanied by a substantial increase in lipid peroxidation. Cell death finally occurred due to DNA damage [13].

4. Conclusion

We report in this work the synthesis of stable anatase-crystallized nanoparticles in aqueous medium at low temperature. The organic function grafted on the particle surface improves the dispersion in the liquid carrier. As proven by our photocatalytic studies, our TiO₂ nanoparticles suspension is effective in promoting the chemical

degradation of an organic compound. Concerning the bactericidal effect of the TiO₂ nanoparticles produced, the bactericidal kinetic is highly correlated to the dispersion state of the TiO₂ nanoparticles in the medium. The use of suspension of TiO₂ nanoparticles in the carrying liquid is much more efficient than the TiO₂ nanopowder. The hybrid titania nanoparticles suspended in aqueous solution have a high specific surface so they provide a better accessibility of TiO₂ nanoparticles to bacteria cells and furthermore leads to faster radical death of micro-organisms under UV irradiation. The hybrid titania nanoparticles suspended in aqueous solution open the way to the synthesis of self-cleaning surfaces, useful in the medical field, pollution removal and functional material.

5. Acknowledgements

The authors acknowledge the University of Auvergne for its financial support. The authors thank Dominique Jalabert and Caroline Andrezza for the HRTEM images (University of Orléans).

REFERENCES

- [1] C. S. Hoffman, P. Mendola, D. Savitz, A. Herring, D. Loomis, K. Hartmann, P. Singer, H. Weinberg and A. Olshan, "Drinking Water Disinfection By-Product Exposure and Fetal Growth," *Epidemiology*, Vol. 19, No. 5, 2008, pp. 729-737. doi:10.1097/EDE.0b013e3181812bd4
- [2] S. Richardson and C. Postigo, "Drinking Water Disinfection By-Products," In: *Emerging Organic Contaminants and Human Health*, Springer, Berlin & Heidelberg, pp. 93-137.
- [3] L. Backer, D. Ashley, M. Bonin, F. Cardinali, S. Kieszak, J. Wooten, *et al.*, "Household Exposures to Drinking Water Disinfection By-Products: Whole Blood Trihalomethane Levels," *Journal of Exposure Analysis and Environmental Epidemiology*, Vol. 10, No. 4, 2000, pp. 321-326. doi:10.1038/sj.jea.7500098
- [4] M. Gosau, S. Hahnel, F. Schwarz, T. Gerlach, T. Reichert and R. Bürgers, "Effect of Six Different Peri-Implantitis Disinfection Methods on *in Vivo* Human Oral Biofilm," *Clinical Oral Implants Research*, Vol. 21, No. 8, 2010, pp. 866-872. doi:10.1111/j.1600-0501.2009.01908.x
- [5] B. Gan, J. Kim, G. Reid, P. Cadieux and J. C. Howard, "Lactobacillus Fermentum RC-14 Inhibits Staphylococcus Aureus Infection of Surgical Implants in Rats," *Journal of Infectious Diseases*, Vol. 185, No. 5, 2002, pp. 1369-1372. doi:10.1086/340126
- [6] J. Reefhuis, M. Honein, C. Whitney, S. Chamany, E. Mann, K. Biernath, K. Broder, S. Manning, S. Avashia, M. Victor, *et al.*, "Risk of Bacterial Meningitis in Children with Cochlear Implants," *New England Journal of Medicine*, Vol. 349, No. 5, 2003, pp. 435-445. doi:10.1056/NEJMoa031101
- [7] K. Kühn, I. Chaberny, K. Massholder, M. Stickler, V. Benz, H. Sonntag and L. Erdinger, "Disinfection of Surfaces by Photocatalytic Oxidation with Titanium Dioxide and UVA Light," *Chemosphere*, Vol. 53, No. 1, 2003, pp. 71-77. doi:10.1016/S0045-6535(03)00362-X
- [8] K. Sunada, T. Watanabe and K. Hashimoto, "Studies on Photokilling of Bacteria on TiO₂ Film," *Journal of Photochemistry and Photobiology*, Vol. 156, No. 1, 2003, pp. 227-233. doi:10.1016/S1010-6030(02)00434-3
- [9] M. Cho, H. Chung, W. Choi and J. Yoon, "Different Inactivation Behaviors of MS-2 Phage and *Escherichia coli* in TiO₂ Photocatalytic Disinfection," *Applied and Environmental Microbiology*, Vol. 71, No. 1, 2005, pp. 270-275. doi:10.1128/AEM.71.1.270-275.2005
- [10] J. Verran, G. Sandoval, N. S. Allen, M. Edge and J. Stratton, "Variables Affecting the Antibacterial Properties of Nano and Pigmentary Titania Particles in Suspension," *Dyes and Pigments*, Vol. 73, No. 3, 2007, pp. 298-304. doi:10.1016/j.dyepig.2006.01.003
- [11] B. Pal, I. Singh, K. Angrish, R. Aminedi and N. Das, "Rapid Photokilling of Gram-Negative *Escherichia coli* Bacteria by Platinum Dispersed Titania Nanocomposite Films," *Materials Chemistry and Physics*, Vol. 136, No. 1, 2012, pp. 21-27.
- [12] G. Rajakumar, A. A. Rahuman, S. M. Roopan, V. G. Khanna, G. Elango, C. Kamaraj, A. A. Zahir and K. Velayutham, "Fungus-Mediated Biosynthesis and Characterization of TiO₂ Nanoparticles and Their Activity against Pathogenic Bacteria," *Spectrochimica Acta Part A*, Vol. 91, 2012, pp. 23-29. doi:10.1016/j.saa.2012.01.011
- [13] A. Kumar, A. K. Pandey, S. S. Singh, R. Shanker and A. Dhawan, "Engineered ZnO and TiO₂ Nanoparticles Induce Oxidative Stress and DNA Damage Leading to Reduced Viability of *Escherichia coli*," *Free Radical Biology and Medicine*, Vol. 51, No. 10, 2011, pp. 1872-1881.
- [14] Y. Xie, Y. He, P. L. Irwin, T. Jin and X. Shi, "Antibacterial Activity and Mechanism of Action of Zinc Oxide Nanoparticles against *Campylobacter jejuni*," *Applied and Environmental Microbiology*, Vol. 77, No. 7, 2011, pp. 2325-2331. doi:10.1128/AEM.02149-10
- [15] R. K. Dutta, B. P. Nenavathu, M. K. Gangishetty and A. V. R. Reddy, "Studies on Antibacterial Activity of ZnO Nanoparticles by ROS Induced Lipid Peroxidation," *Colloids and Surfaces*, Vol. 94, No. 3, 2012, pp. 143-150. doi:10.1016/j.colsurfb.2012.01.046
- [16] J. McCormick, B. Zhao, S. Rykov, H. Wang and J. Chen, "Thermal Stability of Flame-Synthesized Anatase TiO₂ Nanoparticles," *The Journal of Physical Chemistry B*, Vol. 108, No. 45, 2004, pp. 17398-17342. doi:10.1021/jp046874f
- [17] D. Zhao, T. Peng, L. Lu, P. Cai, P. Jiang and Z. Bian, "Effect of Annealing Temperature on the Photoelectrochemical Properties of Dye-Sensitized Solar Cells Made with Mesoporous TiO₂ Nanoparticles," *The Journal of Physical Chemistry C*, Vol. 112, No. 22, 2008, pp. 8486-8494. doi:10.1021/jp800127x
- [18] W. J. Tseng and K. C. Lin, "Rheology and Colloidal Structure of Aqueous TiO₂ Nanoparticle Suspensions," *Materials Science and Engineering: A*, Vol. 355, No. 1, 2011, pp. 186-191. doi:10.1016/S0921-5093(03)00063-7
- [19] M. Kanna and S. Wongnawa, "Mixed Amorphous and

- Nanocrystalline TiO₂ Powders Prepared by Sol-Gel Method: Characterization and Photocatalytic Study,” *Materials Chemistry and Physics*, Vol. 110, No. 1, 2008, pp. 166-175. [doi:10.1016/j.matchemphys.2008.01.037](https://doi.org/10.1016/j.matchemphys.2008.01.037)
- [20] I. Paramasivam, J. M. Macak and P. Schmuki, “Photocatalytic Activity of TiO₂ Nanotube Layers Loaded with Ag and Au Nanoparticles,” *Electrochemistry Communications*, Vol. 10, No. 1, 2008, pp. 71-75. [doi:10.1016/j.elecom.2007.11.001](https://doi.org/10.1016/j.elecom.2007.11.001)
- [21] E. Feschet-Chassot, V. Raspal, Y. Sibaud, O. K. Awitor, F. Bonnemoy, J. L. Bonnet and J. Bohatier, “Tunable Functionality and Toxicity Studies of Titanium Dioxide Nanotube Layers,” *Thin Solid Films*, Vol. 519, No. 8, 2011, pp. 2564-2568. [doi:10.1016/j.tsf.2010.12.184](https://doi.org/10.1016/j.tsf.2010.12.184)
- [22] Y.-H. Tsuang, J.-S. Sun, Y.-C. Huang, C.-H. Lu, W. H.-S. Chang and C.-C. Wang, “Studies of Photokilling of Bacteria Using Titanium Dioxide Nanoparticles,” *Artificial Organs*, Vol. 32, No. 2, 2008, pp. 167-147. [doi:10.1111/j.1525-1594.2007.00530.x](https://doi.org/10.1111/j.1525-1594.2007.00530.x)
- [23] M. Cho, H. Chung, W. Choi and J. Yoon, “Linear Correlation between Inactivation of *E. coli* and OH Radical Concentration in TiO₂ Photocatalytic Disinfection,” *Water Research*, Vol. 38, No. 4, 2004, pp. 1069-1077. [doi:10.1016/j.watres.2003.10.029](https://doi.org/10.1016/j.watres.2003.10.029)
- [24] L. K. Adams, D. Y. Lyon and P. J. J. Alvarez, “Comparative Eco-Toxicity of Nanoscale TiO₂, SiO₂, and ZnO Water Suspensions,” *Water Research*, Vol. 40, No. 19, 2006, pp. 3527-3532. [doi:10.1016/j.watres.2006.08.004](https://doi.org/10.1016/j.watres.2006.08.004)
- [25] G. Bringmann and R. Kuehn, “Comparison of the Toxicity Thresholds of Water Pollutants to Bacteriae, Algae and Protozoa in the Cell Multiplication Inhibition Test,” *Water Research*, Vol. 14, No. 3, 1980, pp. 231-241. [doi:10.1016/0043-1354\(80\)90093-7](https://doi.org/10.1016/0043-1354(80)90093-7)
- [26] X.-B. Chen, W.-H. Fang and D. L. Phillips, “Theoretical Studies of the Photochemical Dynamics of Acetylacetone: Isomerization, Dissociation, and Dehydration Reactions,” *Journal of Physical Chemistry A*, Vol. 110, No. 13, 2006, pp. 4434-4441. [doi:10.1021/jp057306i](https://doi.org/10.1021/jp057306i)